Official journal of the American Society of Gene & Cell Therapy

MTOpen

Cardiac Nerve Growth Factor Overexpression Induces Bone Marrow–derived Progenitor Cells Mobilization and Homing to the Infarcted Heart

Marco Meloni[1,2,9], Daniela Cesselli[3], Andrea Caporali[1,4], Giuseppe Mangialardi[1], Elisa Avolio[1,3], Carlotta Reni[1], Orazio Fortunato[5], Stefania Martini[3], Paolo Madeddu[1], Marco Valgimigli[6], Evgeni Nikolaev[7], Leszek Kaczmarek[7], Gianni D Angelini[1], Antonio P Beltrami[3] and Costanza Emanueli[1,8]

[1]Bristol Heart Institute, School of Clinical Sciences, University of Bristol, Bristol, UK; [2]Institute of Cardiovascular and Medical Sciences, BHF Glasgow Cardiovascular Research Centre, University of Glasgow, Glasgow, UK; [3]Department of Medical and Biological Sciences, University of Udine, Udine, Italy; [4]BHF Centre for Cardiovascular Science, University of Edinburgh, Edinburgh, UK; [5]IRCCS Multimedica, Milan, Italy; [6]Cardiology Department, University of Ferrara, Ferrara, Italy; [7]Laboratory of Molecular Neurobiology, Nencki Institute, Warsaw, Poland; [8]National Heart and Lung Institute, Imperial College London, London, UK; [9]Current address: BHF Centre for Cardiovascular Science, University of Edinburgh, Edinburgh, UK

Reparative response by bone marrow (BM)-derived progenitor cells (PCs) to ischemia is a multistep process that comprises the detachment from the BM endosteal niche through activation of osteoclasts and proteolytic enzymes (such as matrix metalloproteinases (MMPs)), mobilization to the circulation, and homing to the injured tissue. We previously showed that intramyocardial nerve growth factor gene transfer (NGF-GT) promotes cardiac repair following myocardial infarction (MI) in mice. Here, we investigate the impact of cardiac NGF-GT on postinfarction BM-derived PCs mobilization and homing at different time points after adenovirus-mediated NGF-GT in mice. Immunohistochemistry and flow cytometry newly illustrate the temporal profile of osteoclast and activation of MMP9, PCs expansion in the BM, and liberation/homing to the injured myocardium. NGF-GT amplified these responses and increased the BM levels of active osteoclasts and MMP9, which were not observed in MMP9-deficient mice. Taken together, our results suggest a novel role for NGF in BM-derived PCs mobilization/homing following MI.

Received 26 February 2015; accepted 12 August 2015; advance online publication 6 October 2015. doi:10.1038/mt.2015.167

INTRODUCTION

The bone marrow (BM) contains different types of progenitor cells (PCs), which are distributed in the osteoblastic (also known as endosteal) and the vascular niches.[1,2] In physiologic conditions, a relatively small number of stem/PCs are released from the BM into the circulation, together with mature hematopoietic cells.[3] While the latter ensure the regular turnover of circulating leukocytes, erythrocytes, and platelets, the former are supposed to participate in maintaining the integrity of the peripheral vasculature. The homeostatic control of mobilization involves retaining and releasing mechanisms within the BM and modulatory influences from the extra-BM environment. Following an acute ischemic event, such as myocardial infarction (MI), this homeostasis is disrupted leading to an abundant release of immature and maturing hematopoietic cells into the circulation, followed by homing to the ischemic tissue.[4,5] The short-term availability of immature cells to peripheral organs is thought to be a specialized host defense response, contributing to postischemic healing through stimulation of vascularization of the injured tissue. Recent reports have shown that mobilization of vascular PCs from the BM requires many complex signals that concur in detaching the PCs from the stroma. Some cytokines (including the c-kit ligand stem cell factor (SCF),[6] the granulocyte colony–stimulating factor (G-CSF),[7] stromal cell–derived factor-1 (SDF-1),[8,9] and angiogenic factors such as vascular endothelial growth factor A[9,10]) have been shown to activate the release of proteolytic enzymes, including matrix metalloproteinases (MMPs) and cathepsins, which cleave the membrane-bound c-kit ligand, SCF, and other components of the extracellular matrix that normally support the adhesion of stem cells to the niche.[3,11,12] Osteoclasts are a rich source of MMPs, cathepsins, and other mobilizing cytokines, such as interleukin-8.[13,14]

Nerve growth factor (NGF) is a secreted glycoprotein with proangiogenic and antiapoptotic properties.[15–17] Previous data from our laboratory indicate that: (i) NGF expression is increased in the heart of human subjects who died early after a MI, (ii) local adenovirus (*Ad*)-mediated *NGF* gene transfer (GT) promotes post-MI vascular regeneration and myocardial protection resulting in increased post-MI survival and improved cardiac function in mice, and (iii) cardiac *Ad*-mediated *NGF* overexpression is associated with the expansion of Lineage negative (Lin^{neg})/c-kit^{pos} PCs in the mouse left ventricle (LV).[15] Following the latter findings, we aimed to investigate whether therapeutically induced increases in cardiac NGF levels stimulates the mobilization of PCs from the BM and their homing to the infarcted heart, thus contributing to myocardial healing. This study has characterized, for

Correspondence: Costanza Emanueli, Bristol Heart Institute, School of Clinical Sciences, University of Bristol, Bristol Royal Infirmary, Bristol BS2 8HW, UK. E-mail: c.emanueli@yahoo.co.uk or Marco Meloni, BHF Glasgow Cardiovascular Research Centre, University of Glasgow, Glasgow G12 8TA, UK. E-mail: Marco.Meloni@glasgow.ac.uk

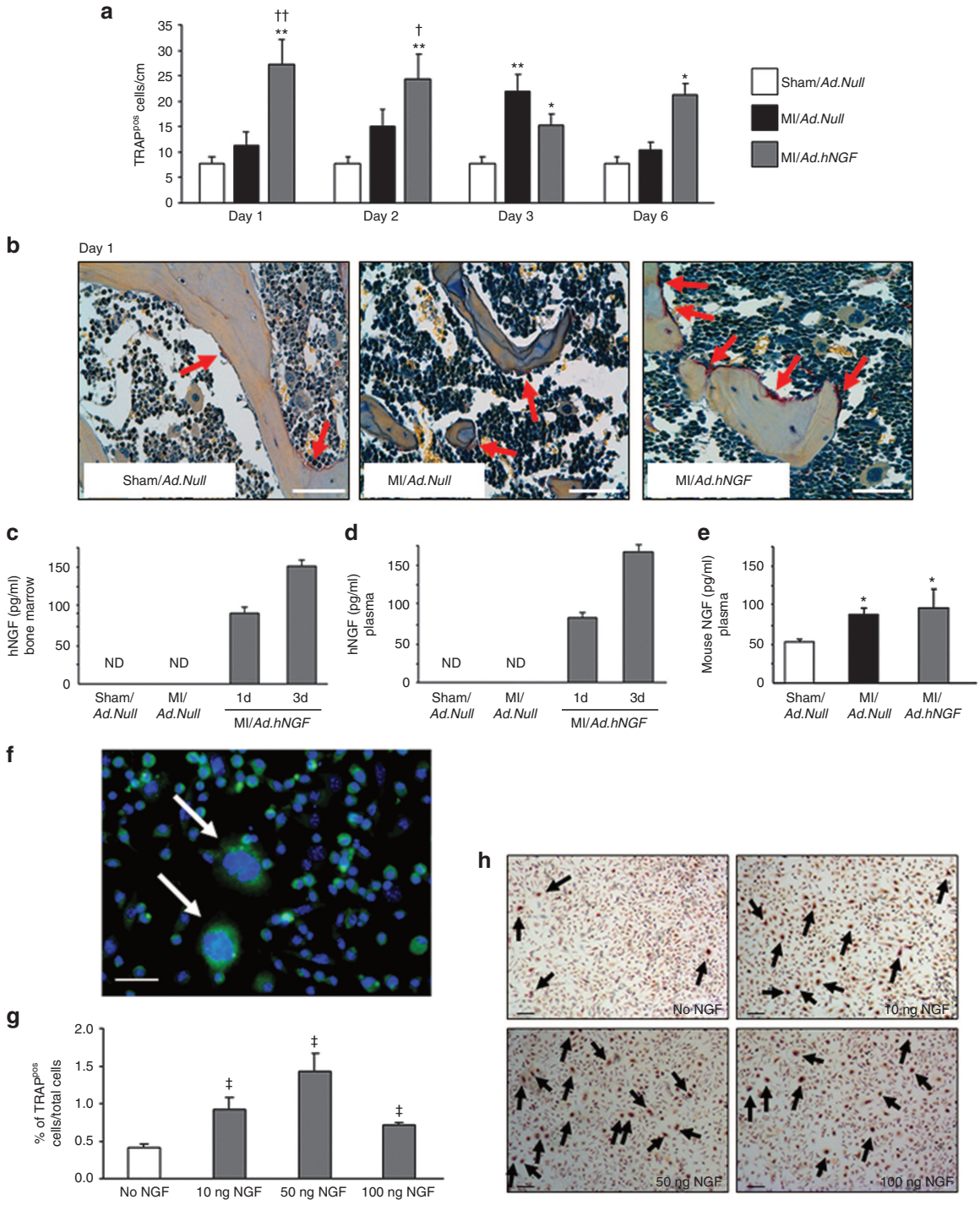

Figure 1 Effects of NGF on osteoclast activation. (**a**) Mouse femurs and tibiae were collected at 1, 2, 3, and 6 days after surgery. Bar graph shows the kinetics of osteoclast activation up to 6 days postsurgery and cardiac gene transfer (GT). Data are expressed as number of TRAP^{pos} osteoclasts/cm of endosteal bone. (**b**) Representative microphotographs of TRAP^{pos} osteoclasts (in purple and pointed by arrows) at 1 day after surgery and GT. Bar = 100 µm. Bar graphs show the presence of *hNGF* restricted to the (**c**) bone marrow (BM) supernatant and (**d**) peripheral blood plasma of mice that received cardiac *Ad.hNGF*-GT. Analyses were performed at 1 and 3 days postsurgery and GT (n = 3–4/group). (**e**) ELISA for endogenous NGF in the mouse peripheral blood plasma at 3 days postsurgery (n = 6/group). (**f**) Representative microphotograph showing the presence of NGF high-affinity receptor TrkA (green fluorescence) in terminally differentiated multinucleated osteoclasts (pointed by arrows). Nuclei are stained by 4′,6-diamidino-2-phenylindole (blue fluorescence). Bar = 20 µm. (**g**) Bar graphs show the effect of NGF on TRAP expression in murine BM-derived mononuclear cells (MNCs) undergoing osteoclast differentiation. Data are expressed as percentage of TRAP^{pos} osteoclasts/total cells. (**h**) Representative microphotographs of TRAP^{pos} cells (in red and pointed by arrows) at 6 days after treatment with NGF. Bar = 100 µm. Data are expressed as mean ± SEM. *P < 0.05 and **P < 0.01 versus sham/*Ad.Null*; $^{\dagger}P$ < 0.05 and $^{\dagger\dagger}P$ < 0.01 versus MI/*Ad.Null*; $^{\ddagger}P$ < 0.05 versus no NGF (n = 5 samples/group for TRAP staining on mouse bones and 3 samples/group for TRAP staining on isolated mouse MNCs). *Ad*, adenovirus; hNGF, human nerve growth factor; MI, myocardial infarction; N.D., not detectable; TRAP, tartrate-resistant acid phosphatase.

the first time, the time-course of osteoclasts activation and BM c-kit^{pos} cell expansion in response to MI. Moreover, we provide novel evidence supporting the hypothesis that after *Ad*-mediated intracardiac delivery of human *NGF*, the transgenic NGF reaches the BM, where it activates osteoclasts that in turn trigger MMP9 activation and SCF release. These pathways lead to increased c-kit^{pos} cells egress from the BM and their homing to the infarcted heart and are associated with improved myocardial blood flow and cardiac function in mice receiving NGF-GT.

RESULTS

NGF induces osteoclast activation and increases MMP9-positive cells in the BM

Osteoclasts typically reside in endosteal pits and derive from the fusion of monocytes through a reaction that is triggered by receptor activator of NF-κB ligand (RANKL) and macrophage colony–stimulating factor (M-CSF) and involves the transcription factor NF-κB.[18] Firstly, we investigated the effect of MI and concomitant NGF cardiac overexpression on osteoclast activation. For this purpose, a mouse model of MI induced by permanent ligation of the left anterior descending coronary artery[15,19] was employed. Following MI induction, mice received intracardiac injections of either *Ad.hNGF* or an empty vector (*Ad.Null*, used as control of NGF-GT as well as to characterize the BM response to MI in the absence of a gene therapy intervention). Sham-operated mice receiving *Ad.Null* served for reference. At 1, 2, 3, and 6 days after the intervention, the abundance of acid phosphatase-rich osteoclasts in the femurs and tibias was assessed by immunohistochemistry for tartrate-resistant acid phosphatase (TRAP). As shown in **Figure 1**, in *Ad.Null*-given mice, the number of TRAP^{pos} active osteoclasts lining the endosteal surface was increased at 3 days post-MI compared to sham operation. This change was transient (not observable at 6 days), thus suggesting that osteoclast activation is not sustained by MI alone. Of note, assessment of TRAP^{pos} osteoclasts in bones collected from MI or sham-operated mice receiving phosphate-buffered saline showed similar results, thus excluding the possibility of an *Ad*-mediated effect on osteoclast activation (data not shown). Remarkably, intramyocardial *Ad.hNGF* increased the number of TRAP^{pos} osteoclasts already at 1 and 2 days post-MI, thus accelerating osteoclast activation in comparison to the *Ad.Null* group (**Figure 1a**,**b**). Moreover, after NGF-GT, osteoclast activation was sustained up to the last time point (6 days post-MI) of this protocol (**Figure 1a**). In order to verify if the transgenic human protein reaches the BM through the circulation, we employed an enzyme-linked immunosorbent assay (ELISA) selective for hNGF. Human NGF was measured in the peripheral blood (PB)-derived plasma and BM supernatants at 1 and 3 days post-GT in MI mice. In mice receiving NGF-GT, hNGF was present in both plasma and BM, whereas hNGF could not be detected in *Ad.Null*-given mice (**Figure 1c**,**d**, respectively). In addition, the levels of endogenous (mouse) NGF also increased in the plasma of infarcted mice, but no further increase was observed after *hNGF*-GT (**Figure 1e**).

Next, to determine if osteoclasts could be a cellular target for hNGF, the expression of the NGF high-affinity receptor TrkA on osteoclasts derived from *in vitro* differentiation of mouse BM-derived mononuclear cells (BM-MNCs) was assessed by immunocytochemistry. As shown in **Figure 1f**, terminally differentiated multinucleated osteoclasts (which have a larger size in comparisons to their MNC precursors) stained positive for TrkA. Moreover, using an *in vitro* osteoclast differentiation assay, we found that hNGF potentiates the effect of M-CSF and RANKL, which are the natural activators of osteoclast formation[20] (**Figure 1g**,**h**).

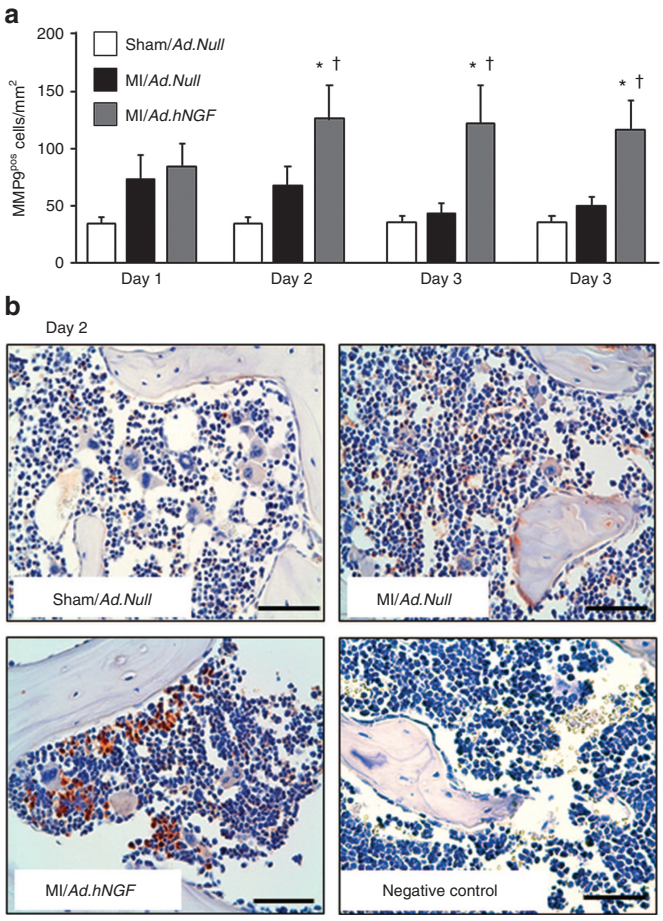

Figure 2 NGF-dependent increase of MMP9 in the mouse bone marrow (BM) after MI and gene transfer (GT). (**a**) Bar graph shows the expression of MMP9 in the mouse BM parenchyma up to 6 days postsurgery and cardiac GT. Data are expressed as number of MMP9^{pos} cells/mm^2 of BM parenchyma. (**b**) Representative microphotographs of MMP9^{pos} BM cells (in brown) at 2 days postsurgery and GT. Bar = 50 µm. Data are expressed as mean ± SEM. *P < 0.05 versus sham/*Ad.Null*; †P < 0.05 versus MI/*Ad.Null* (n = 5 samples/group). *Ad*, adenovirus; hNGF, human nerve growth factor; MI, myocardial infarction; MMP, matrix metalloproteinase.

Osteoclasts are a rich source of proteolytic enzymes, which facilitate the detachment of stem/PCs from the extracellular matrix.[14] We found that, although MI alone does not affect the BM level of active MMP9, *hNGF* gene therapy increases the number of cells expressing the active form of MMP9 lining the trabecular bone of infarcted mice up to 6 days (**Figure 2a**,**b**). In contrast, although MI increased the number of MMP2^{pos} cells, no difference was observed after NGF treatment (**Figure 3a**,**b**).

MMP9 is involved in stem/PC mobilization by shedding the membrane-bound cytokine SCF within the BM and releasing this cytokine into the circulation.[6] Therefore, we next sought to evaluate the effect of *hNGF* overexpression on SCF levels in the BM

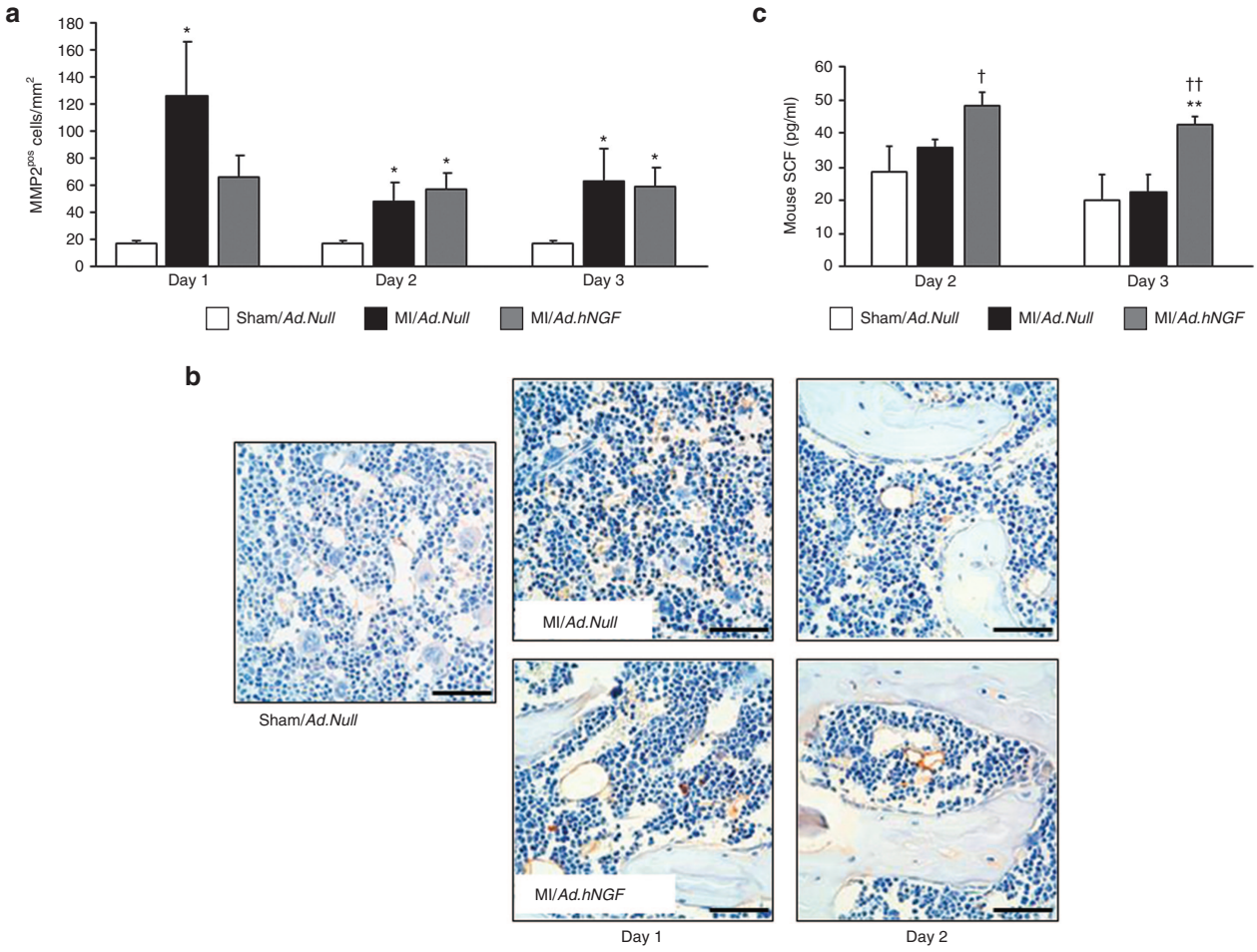

Figure 3 Effects of NGF on MMP2 and SCF in the mouse bone marrow (BM) after MI and gene transfer. (**a**) Bar graph shows the expression of MMP2 in the mouse BM parenchyma at 1, 2, and 3 days following MI (or sham operation) and gene therapy. Data are expressed as number of MMP2^{pos} cells/mm^2 of BM parenchyma. (**b**) Representative microphotographs of MMP2^{pos} BM cells (in brown) at 1 and 2 days postsurgery and gene therapy. Bar = 100 µm. (**c**) Bar graphs show the expression level of SCF (measured by ELISA) in the mouse BM supernatant at 2 and 3 days after surgery and cardiac gene therapy. Data are expressed as mean ± SEM. *$P < 0.05$ and **$P < 0.01$ versus sham/*Ad.Null*; $^{\dagger}P < 0.05$ and $^{\dagger\dagger}P < 0.01$ versus MI/*Ad.Null* ($n = 5$ samples/group for MMP2 staining and 4 samples/group for ELISA assay). *Ad*, adenovirus; hNGF, human nerve growth factor; MI, myocardial infarction; MMP, matrix metalloproteinase; SCF, stem cell factor.

supernatants of infarcted mice. Results show that MI induces a modest increase in SCF levels, with this effect being remarkably enhanced in infarcted mice receiving cardiac NGF-GT (**Figure 3c**).

NGF increases the abundance of c-kit^{pos} cells in the BM

Next, we investigated the relationship between NGF-induced activation of the MMP9-SCF pathway and stem/PCs abundance and release. By immunohistochemical analyses, we found that NGF overexpression increased the number of total c-kit^{pos} cells, and of c-kit^{pos}/CD45$^{low/neg}$ and c-kit^{pos}/CD45^{pos} cells in the mouse BM at 3 days post-MI (**Figure 4a–d**). We additionally observed that NGF-GT differently impacts on the localization of c-kit^{pos} cells within the BM endosteal and vascular niches: in fact, whereas the relative number of c-kit^{pos} cells lining on the bone surface was not affected by NGF-GT (**Figure 5a**), the relative abundance of c-kit^{pos} cells was found to be increased in proximity of the BM vascular niche (identified by staining for CD146) of *Ad.hNGF*-injected mice (**Figure 5b,c**). Moreover, the percentage of c-kit^{pos}/Ki67^{pos} proliferating cells in the BM was increased by NGF-GT at 3 days post-MI (**Figure 5d,e**). Similarly, flow cytometry analyses on total BM isolated at 3 days post-MI confirmed the increased percentage of c-kit^{pos} cells in *Ad.hNGF*-injected mice (**Figure 5f**). To investigate if the proliferation of c-kit^{pos} cells is induced by NGF directly or through increased SCF,[21,22] c-kit^{pos} cells were isolated from the mouse BM using magnetic-activated cell sorting columns. Next, the expression of the NGF high-affinity receptor TrkA in the isolated c-kit^{pos} cells was assessed by immunocytochemistry. In line with our previous findings on c-kit^{pos} cells from the mouse infarcted heart,[15] we observed that murine BM c-kit^{pos} cells do not express the TrkA receptor (data not shown), thus suggesting that, in mice, the NGF-induced enhancement of c-kit^{pos} cells is attributable to indirect mechanisms that are instead mediated through SCF.

NGF-dependent mobilization of BM-PCs and homing to the MI heart is dependent on MMP9 activation

We next sought to investigate the implication of MMP9 in the NGF-induced effects on BM-PCs (BM-derived PCs).

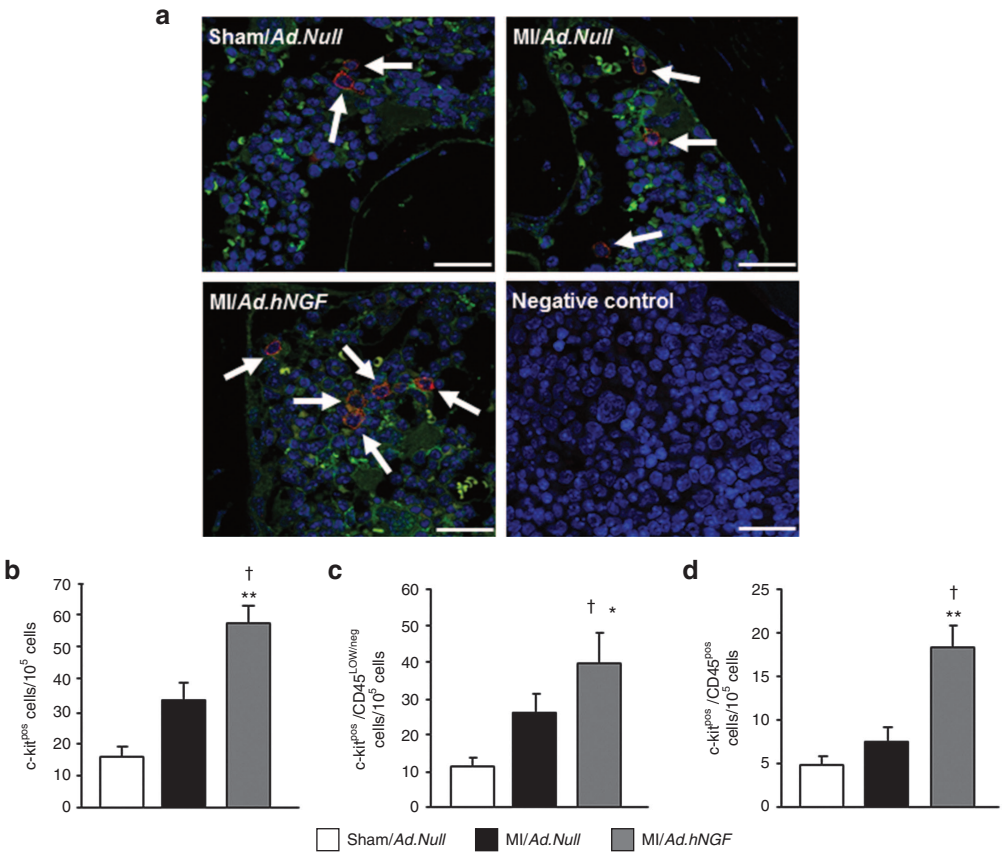

Figure 4 Effect of cardiac NGF gene therapy on c-kit^{pos} progenitor cells in the mouse bone marrow (BM). (**a**) Immunofluorescence staining for c-kit (red fluorescence) and CD45 (green fluorescence) in the mouse BM at 3 days post-MI and gene therapy. White arrows indicate c-kit^{pos} cells. Bar = 25 µm. Bar graphs indicate the number of (**b**) c-kit^{pos} cells, (**c**) c-kit^{pos}/CD45$^{low/neg}$ cells, (**d**) and c-kit^{pos}/CD45^{pos} cells (all expressed as number of positive cells/10^5 total BM cells) at 3 days after surgery and gene transfer. Data are expressed as mean ± SEM. *P < 0.05 and **P < 0.01 versus sham/*Ad.Null*; †P < 0.05 versus MI/*Ad.Null*. All analyses were performed at 3 days postsurgery (n = 5 mice/group). *Ad*, adenovirus; hNGF, human nerve growth factor; MI, myocardial infarction.

Intramyocardial delivery of either *Ad.hNGF* or *Ad.Null* were performed in *MMP9* knockout (KO) and C57BL/6 mice (control wild-type mice on same genetic background as *MMP9* KO) after inducing MI or sham operation. Similarly to what previously observed in CD1 mice,[15] cardiac flow cytometry analyses performed in the C57BL/6 wild-type mice confirmed an increase of Lin^{neg}/c-kit^{pos} cells at 3 days post-MI, with this effect being further incremented by NGF-GT (**Figure 6a–e**). The number of Lin^{neg}/c-kit^{pos} cells was similar in the infarcted hearts of *MMP9* KO mice and wild-type controls. However, *MMP9* deletion was associated with a reduction of the inductive effect of NGF on Lin^{neg}/c-kit^{pos} cells (**Figure 6a–e**), thus suggesting that NGF elicits its effect on BM-PC mobilization and/or PC homing to the infarcted heart *via* a MMP9-dependent mechanism. This is in line with previous report showing NGF to increase MMP9, and MMP9 contributes to NGF effects in different cells.[23,24] Similar to what observed in CD1 mice, the percentage of c-kit^{pos}/Ki67^{pos} proliferating cells in the BM of C57BL6/J mice was enhanced by *Ad.hNGF* after MI but remained unchanged in *MMP9* KO mice (data not shown). Interestingly, the percentage of Lin^{neg}/c-kit^{pos} cells in the PB at 3 days post-MI was significantly enhanced by *Ad.hNGF* in wild-type mice but it was blunted by *MMP9* deletion (**Figure 6f**).

BM origin of c-kit^{pos} cells after NGF-GT in mice with MI

In order to investigate the BM origin of the lin^{neg}/c-kit^{pos} cells enriched in the infarcted mouse heart by cardiac NGF-GT, we used a mouse model of BM transplantation. C57BL/6-Tg[CAG-EGFP]1Osb/J, carrying an enhanced green fluorescent protein (eGFP), were used as donors and C57BL6/J as recipient mice (**Figure 7a**). Success of BM transplantation was confirmed by flow cytometry analysis of PB collected at 8 weeks after GFP-BM cells transplantation (**Figure 7b–d**). Fluorescent intensity showed that 69 ± 6% of all nucleated cells expressed the fluorescent marker, indicating successful replacement of the BM cells population. Cardiac flow cytometry performed at 3 days post-MI and GT showed increased abundance of BM-derived Lin^{neg}/c-kit^{pos}/GFP^{pos} cells into the infarcted heart treated with *Ad.hNGF* (**Figure 7e–k**), thus providing evidence of the capacity of NGF to attract BM-PCs to the infarcted heart.

NGF is a chemoattractant for human BM- and PB-derived MNCs

Contrarily to mouse c-kit^{pos} cells, human c-kit^{pos} cells possess TrkA receptor for NGF and therefore they might use this receptor to directly respond to an NGF stimulus. As shown in **Figure 8a–c**,

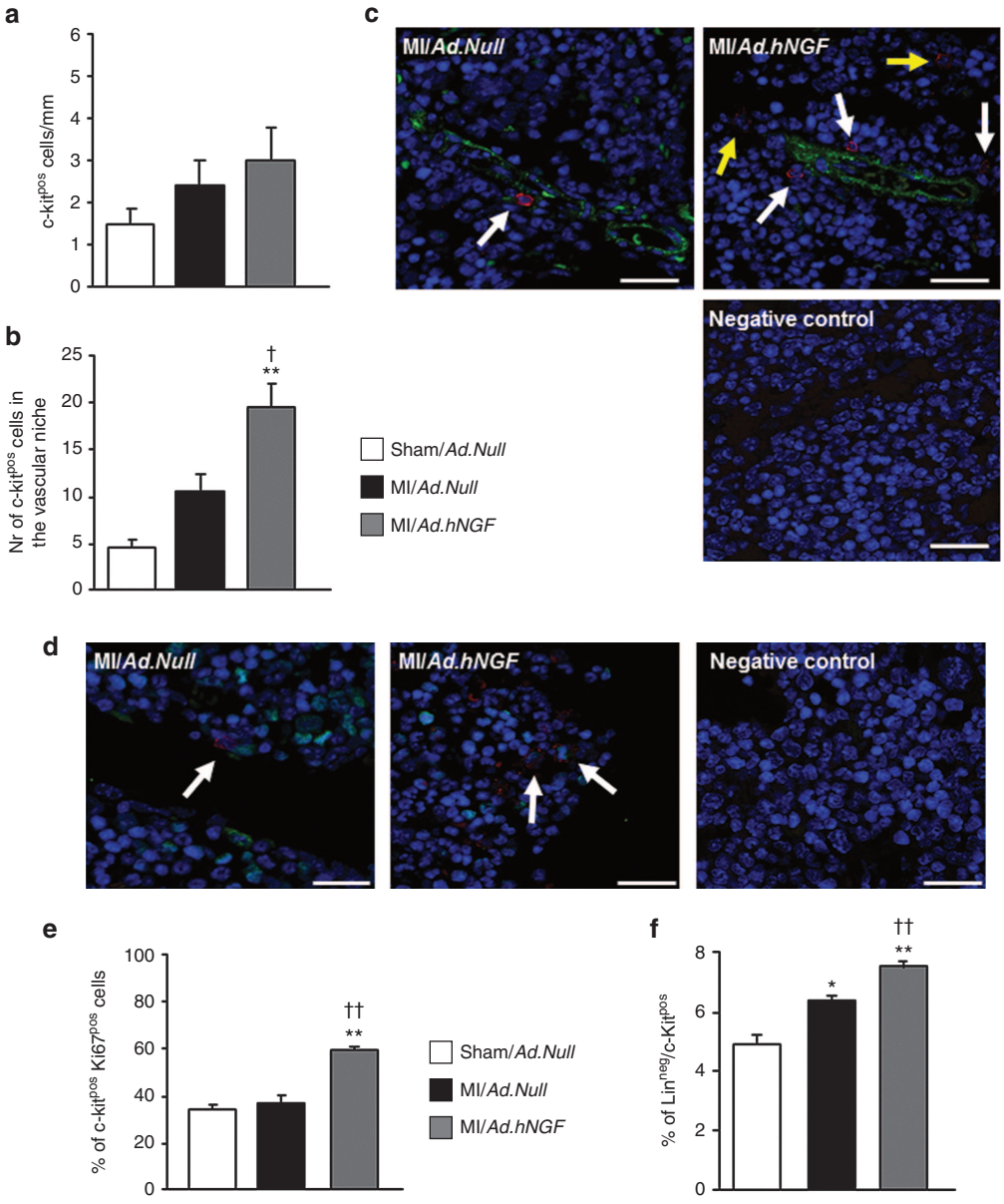

Figure 5 Effect of cardiac NGF gene therapy on c-kit^{pos} cells localization in the mouse bone marrow (BM). Bar graphs shows (**a**) number of c-kit^{pos} cells lining on the BM endosteal region and (**b**) number of c-kit^{pos} cells in proximity to the vascular niche. (**c**) Representative microphotographs of c-kit^{pos} cells (red fluorescence) in the proximity of the BM vascular niche (identified by staining for CD146, green fluorescence). c-kit^{pos} cells close to the vascular niche are pointed by white arrows while c-kit^{pos} cells that are distant from the vascular niche are indicated by yellow arrows. Bar = 25 µm. (**d**) Immunohistochemical staining for c-kit (red fluorescence) and the proliferative marker Ki67 (green fluorescence) in the BM showing increased proliferation of c-kit^{pos} cells induced by *Ad.hNGF* at 3 days after MI and gene therapy (**e**); Bar = 25 µm. Nuclei are stained by 4′,6-diamidino-2-phenylindole (blue fluorescence). (**f**) Quantification of Lin^{neg}/c-kit^{pos} cells by flow cytometry in the BM of mice at 3 days post-MI and gene transfer. Data are expressed as mean ± SEM. *$P < 0.05$ and **$P < 0.01$ versus sham/*Ad.Null*; †$P < 0.05$ and ††$P < 0.01$ versus MI/*Ad.Null*. All analyses were performed at 3 days postoperation ($n = 5$ mice/group). *Ad*, adenovirus; hNGF, human nerve growth factor; MI, myocardial infarction.

flow cytometry confirmed the presence of Lin^{neg}/c-kit^{pos}/TrkA^{pos} cells within the human BM-MNCs. In order to evaluate the potential effect of NGF on human BM-MNCs, cells were subjected to a Transwell migration assay using NGF as chemoattractant. As shown in **Figure 8d**, NGF attracted human BM-MNCs similarly to what observed with SDF-1 (positive control) treatment. Furthermore, flow cytometry analyses showed that NGF migration enriched for CD34^{pos}/c-kit^{pos} and CD34^{pos}/c-kit^{pos}/TrkA^{pos} cells (calculated as ratio of migrated to nonmigrated cells), suggesting that NGF was able to attract these BM-PC populations (**Figure 8e**,**f**, respectively). In addition, the NGF-induced BM-PC migration was repressed by the TrkA inhibitor K252a.

TrkA-expressing BM-derived CD34^{pos}/c-kit^{pos} cells are increased in the peripheral circulation of patients with acute MI

Flow cytometry analyses on clinical samples showed that the abundance of CD34^{pos}/c-kit^{pos} cells coexpressing the TrkA receptor was increased in the PB of acute MI patients (within 5 days from acute MI)[25] in comparisons with healthy controls (**Figure 8g**).

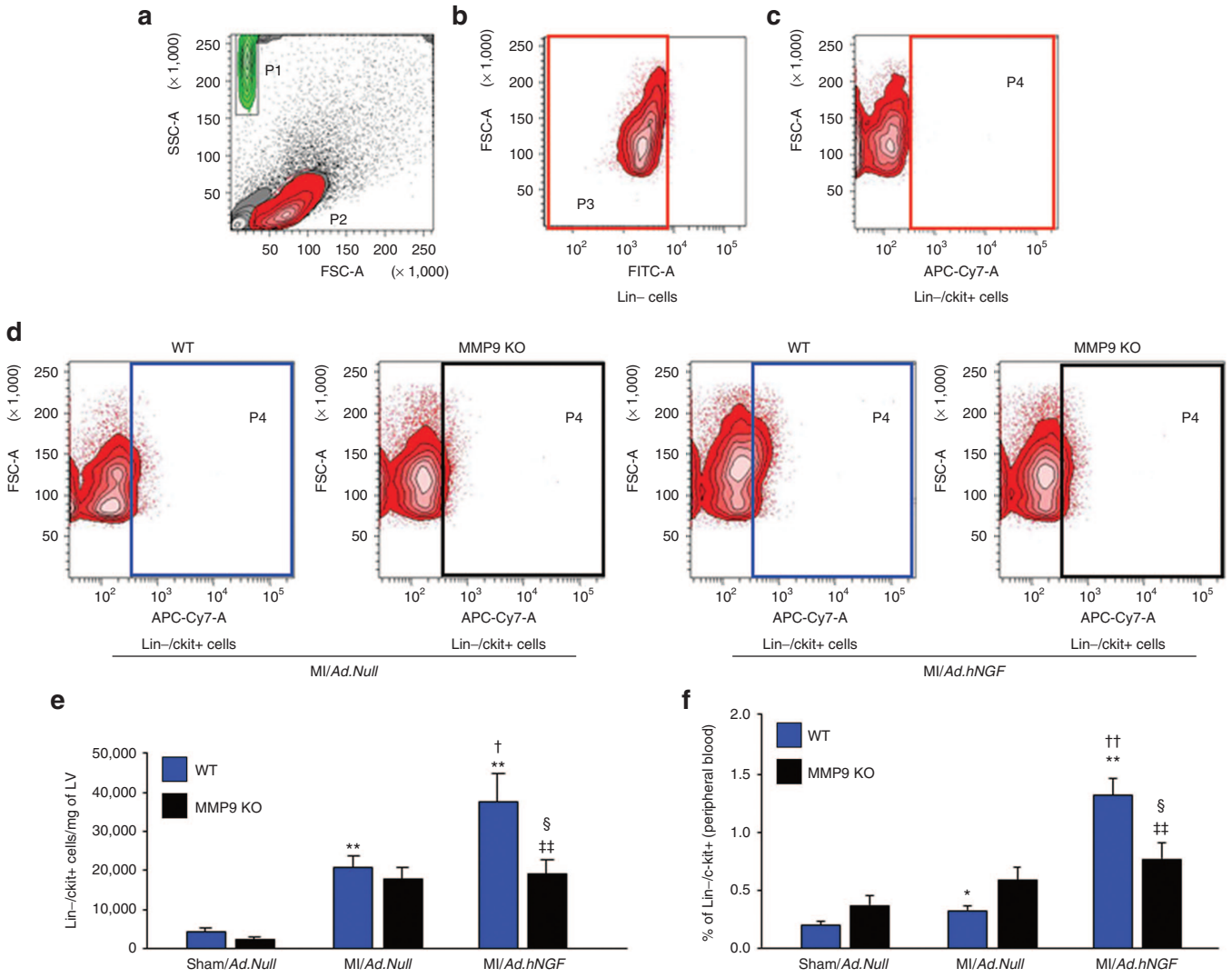

Figure 6 Involvement of MMP9 in the NGF-induced mobilization of bone marrow–derived progenitor cells. Identification and quantification of Lin^{neg}/c-kit^{pos} cells by cardiac flow cytometry in *MMP9* KO and WT (C57BL6/J) mice. (**a**) Forward and side scatter shows the total population (P2, in red) analyzed after LV digestion. For data analysis, counting beads (P1, green) were identified by their size. (**b**) Lin^{neg} cells (P3) were gated from the total population of extracted cells. (**c**) Negative control for c-kit^{pos} cells (P4). Representative (**d**) dot plots and (**e**) bar graphs show the number of Lin^{neg}/c-kit^{pos} cells/mg of LV tissue in MI hearts of WT mice (blue bars) and *MMP9* KO mice (black bars) injected with *Ad.hNGF*. (**f**) Bar graphs show Lin^{neg}/c-kit^{pos} cells mobilization in the peripheral blood (analyzed by flow cytometry). Data are expressed as mean ± SEM. $^{*}P < 0.05$ and $^{**}P < 0.01$ versus WT sham/*Ad.Null*; $^{\dagger}P < 0.05$ and $^{\dagger\dagger}P < 0.01$ versus WT MI/*Ad.Null*; $^{\ddagger}P < 0.01$ versus WT MI/*Ad.hNGF*; $^{\S}P < 0.05$ versus MMP9 KO sham/*Ad.Null*. All analyses were performed at 3 days postoperation ($n = 5$ mice/group). *Ad*, adenovirus; hNGF, human nerve growth factor; KO, knockout; LV, left ventricle; MI, myocardial infarction; MMP, matrix metalloproteinase; WT, wild-type.

Characteristics of acute MI patients and control subjects are shown in **Supplementary Table S1**.

DISCUSSION

Meta-analysis reports indicate that autologous transplantation of BM-MNCs produces modest improvement in LV function in acute MI patients.[26] However, the uniformly null findings emerging from the most recent trials open new controversies in this already troubled field of clinical research.[26] Another experimental approach for stem/PCs–mediated therapy of MI consists of acute stem/PCs mobilization from the BM using G-CSF or equivalent chemokines. However, a recent systematic review of G-CSF clinical trials does not support this approach to produce substantial therapeutic benefit in MI patients.[27] Besides G-CSF, other chemokines and growth factors (such as vascular endothelial growth factor, erythropoietin, fibroblast growth factor, and insulin-like growth factor) have been shown to induce BM-PCs mobilization and promote cardiac repair following MI. However, besides promising preclinical data, randomized, controlled clinical trials showed contrasting results and these factors necessitate of further investigation.[28] Indeed, depending on the dose, as well as the timing of administration, chemokines and growth factors can either induce or have no effect on BM-PCs mobilization.[28] Of note, another approach consisting of G-CSF–mediated mobilization of BM-PCs together with concomitant PC therapy showed conflicting results.[29,30] In fact, despite the favorable effects of G-CSF therapy with concomitant intracoronary infusion of PCs on cardiac function and angiogenesis, aggravation of restenosis or recurrent MI was observed in several

MI patients.[29,30] Nonetheless, it is likely that PC mobilizing factors (over)expressed (by local gene therapy) and released by the infarcted heart for a sufficient time frame which overlaps with the "therapeutic window" could continuously recruit BM-PCs to the myocardium, thus producing meaningful therapeutic results. We were the first to identify the strong therapeutic potential of local NGF-GT in a mouse MI model[15] and we aim to embark in a translational pathway to meet the therapeutic needs of ischemic heart disease patients. Consequently, we are interested in elucidating the full range of mechanisms underpinning the beneficial effect of local NGF delivery. This study was designed to characterize the possible BM responses to cardiac NGF overexpression following MI induction in mice. We have shown that MI *per se* leads to osteoclast activation. Moreover, cardiac NGF-GT expands the BM remodeling responses to MI and is conductive to increase of BM-PCs in the infarcted heart.

Mobilization of PCs from the BM is strictly regulated under either physiological conditions[3,31] or stress situations[5] (such as ischemia or inflammation), it is influenced by different cell types and requires many complex signals. There are three main steps involved in successful migration and engraftment of BM-PCs into the injured tissue: the PCs expansion and translocation from the endosteal niche to the vascular niche, their egress into the circulation, and finally their recruitment into the target organ.[12,32] In the present study, we demonstrate for the first time that NGF is involved in these three steps and in particular that *Ad*-mediated cardiac NGF overexpression induces mobilization of BM-PCs and their homing into the infarcted myocardium in mice.

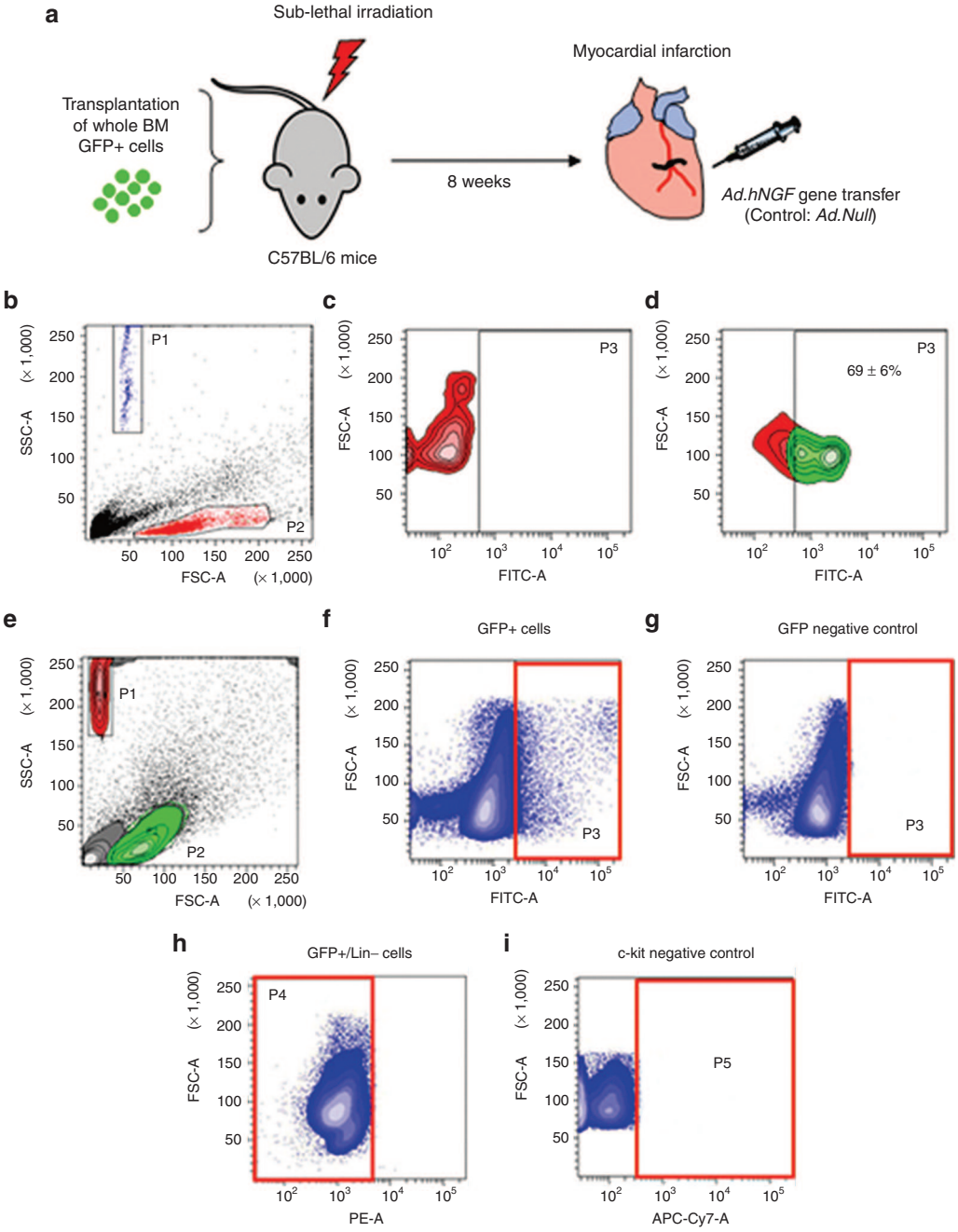

Besides the essential contribution in the regulation of bone reabsorption, osteoclasts have been recently shown to play a significant role in the homeostasis and mobilization of BM-PCs.[1] Osteoclasts derive from the monocyte/macrophage cell lineage and their formation is mainly driven by M-CSF and RANKL.[18,33] Interestingly, a recent study by Hemingway *et al.* demonstrated that NGF, as well as other cytokines, is able to induce osteoclasts formation and activation independently of RANKL.[34] In line with that, here we confirm the ability of NGF to induce the formation of TRAP^{pos} osteoclasts (from BM-MNCs) *in vitro* and we additionally show that terminally differentiated multinucleated osteoclasts possess the NGF receptor TrkA. Of note, higher doses of NGF (100 ng) produce lower effects on murine BM-MNCs undergoing osteoclast differentiation as compared to lower doses (10 and 50 ng). In this context, previous reports indicate that NGF dosage is crucial in determining the extent of its effects[35,36] and we can speculate that high doses of NGF saturate its binding to its high-affinity receptor TrkA and attenuate its effects. This finding might also explain the increased rate of active osteoclasts observed in our *in vivo* model of MI after NGF overexpression. In fact, it is known that several stress signals, including cardiac ischemia, induce and enhance osteoclasts activity[32,37] (as observed here at 3 days after MI and cardiac *Ad.Null* gene therapy). Importantly, we have found that cardiac *Ad.hNGF* gene therapy after MI induces a more rapid and sustained activation of osteoclasts in comparison to MI controls. In turn, osteoclasts activation triggers the secretion of cytokines, proteolytic enzymes (including MMP9), and membrane-bound SCF.[1] Herein, we demonstrate that NGF-induced osteoclasts activation is followed by release of active MMP9 in the mouse BM parenchyma. NGF is known to induce MMP9 expression.[23,38,39] NGF-induced enhanced expression of MMP9 has been shown to promote corneal epithelial cells migration *in vitro* and *in vivo*.[39] In turn, MMP9 plays an important role in BM cell migration. In fact, MMP9 cleaves the cell surface of the soluble c-kit ligand SCF and SCF contributes to the recruitment and mobilization of hematopoietic stem/PCs.[12,40] In the present study, using a KO mouse model, we demonstrate that MMP9 is essential for NGF-induced mobilization of BM-PCs into the circulation and PC homing to the infarcted heart. In fact, by flow cytometry, we found that the frequency of Lin^{neg}/c-kit^{pos} cells in both the PB and the LV of MMP9 KO mice treated with *Ad.hNGF* was reduced and it was comparable to what observed in the PB and infarcted hearts of both wild-type and MMP9 KO mice treated with *Ad.Null*. Most notably, *NGF* gene therapy in infarcted hearts of GFP-BM chimeric mice confirmed the capacity of cardiac NGF overexpression to mobilize and attract BM-PCs to the infarcted heart. The present study, together with our recent findings that NGF promotes cardiac repair after MI,[15] advances the idea that the cardioprotective effect of NGF might be partially mediated by its ability to recruit BM progenitors to the myocardium. Furthermore, we

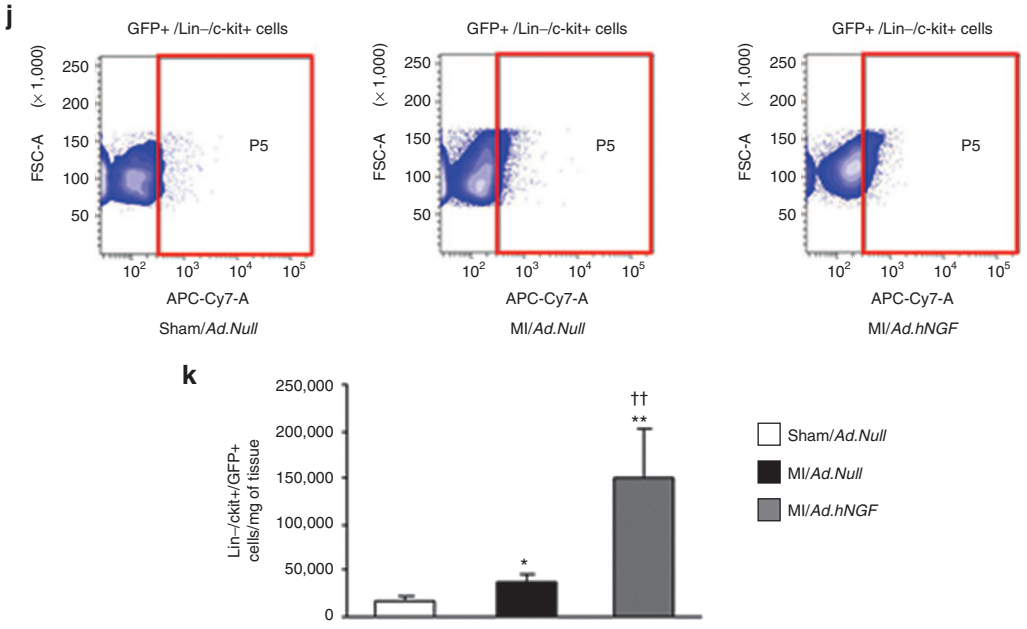

Figure 7 BM transplantation studies. (**a**) Schematic representation of BM transplantation studies: GFP^{pos} cells (in green) were isolated from the BM of GFP^{pos} transgenic mice and subsequently transplanted into sublethally irradiated recipient C57BL/6 mice. After 8 weeks, mice underwent MI and cardiac gene therapy. (**b–d**) Efficacy of BM transplantation evaluated by flow cytometry for GFP on peripheral blood (PB) collected from mice at 6 weeks after sublethal irradiation and transplantation. (**b**) Forward and side scatter shows the total population analyzed (P2, in red). Counting beads (P1, in blue) were used to determine the absolute number of GFP^{pos} cells. (**c**) Negative control for GFP^{pos} cells (P3). GFP^{pos} cells were gated from the total population. (**d**) Fluorescent intensity shows the percentage of all nucleated cells in the PB of chimeric mice that expressed GFP. (**e–i**) Identification and quantification of cardiac GFP^{pos}/Lin^{neg}/c-kit^{pos} cells by flow cytometry. Forward and side scatter (**e**) shows the total population analyzed (P2, in green) after digestion of the left ventricle (LV). Counting beads (P1, in red) were used to determine the absolute number of progenitor cells per gram of LV. (**f**) Distribution of GFP^{pos} cells (in P3) isolated from the LV of a transplanted recipient mouse. (**g**) Negative control for GFP, established using cells isolated from the LV of nontransplanted mice. (**h**) Lin-cells were gated from GFP^{pos} cells (P4). (**i**) Negative control for c-kit. Representative (**j**) dot plots and (**k**) bar graphs show the number of GFP^{pos}/Lin^{neg}/c-kit^{pos} cells/mg of LV tissue after MI and cardiac *Ad.hNGF* treatment. Data are expressed as mean ± SEM. $^{**}P < 0.01$ and $^{*}P < 0.05$ versus Sham/*Ad.Null*; $^{††}P < 0.01$ versus MI/*Ad.Null* ($n = 6$ mice/group). *Ad*, adenovirus; BM, bone marrow; GFP, green fluorescent protein; hNGF, human nerve growth factor; MI, myocardial infarction

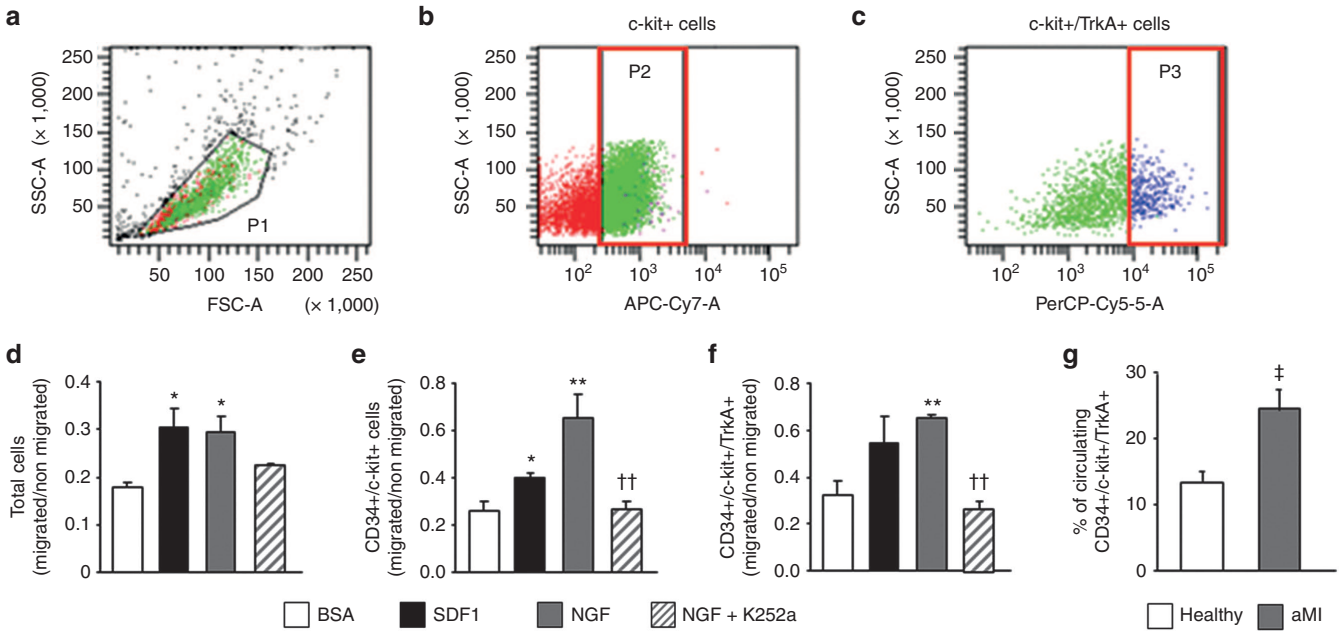

Figure 8 ***In vitro*** **migration of bone marrow (BM)- and peripheral blood (PB)-derived mononuclear cells (MNCs) towards NGF.** (**a–c**) Identification by flow cytometry of c-kit^{pos}/TrkA^{pos} cells in human BM-derived MNCs. (**a**) Forward and side scatter shows the total population analyzed (P1). (**b**) c-kit^{pos} cells (P2) were gated from the total cells population and double-positive cells for c-kit and TrkA (**c**) are shown in P3. (**d–f**) Quantitative analysis of human BM-derived MNCs (obtained from noncardiovascular patients) after *in vitro* Transwell migration towards NGF shows migration of human MNCs (**d**) and enrichment for CD34^{pos}/c-kit^{pos} (**e**) and CD34^{pos}/c-kit^{pos}/TrkA^{pos} (**f**). The TrkA inhibitor K252a was used to repress NGF. (**g**) Bar graphs show the percentage of CD34^{pos}/c-kit^{pos}/TrkA^{pos} cells in the PB of either healthy subjects or patients with an acute MI (within 5 days following MI). BSA and SDF-1 have been used as negative and positive controls, respectively. Data are expressed as mean ± SEM. $^{**}P < 0.01$ and $^{*}P < 0.05$ versus BSA; $^{††}P < 0.01$ versus NGF; $^{‡}P < 0.05$ versus Healthy ($n = 3$ subjects/group for human BM samples and $n = 11$ subjects/group for human PB samples). aMI, acute myocardial infarction; BSA, bovine serum albumin; NGF, nerve growth factor; SDF, stromal cell–derived factor.

have recently revealed that increase of SCF induced by NGF in the MI heart promotes the expansion of cardiac c-kit^{pos} cells.[15] Here, we additionally demonstrate that NGF, possibly through MMP9, leads to SCF increase in the mouse BM, followed by proliferation of c-kit^{pos} PCs in the BM parenchyma.

However, our *in vivo* data suggest that NGF is not able to directly induce PC mobilization from the mouse BM (as mouse c-kit^{pos} cells do not possess the NGF high-affinity receptor TrkA), where MMP9 and SCF appear to be essential. Conversely, TrkA is present on c-kit^{pos} cells isolated from the human BM and it induces their migration *in vitro*, as supported by the fact that the TrkA inhibitor K252a potently suppresses migration of CD34^{pos}/c-kit^{pos} and CD34^{pos}/c-kit^{pos}/TrkA^{pos} cells towards NGF. These results may have clinical relevance for the treatment of ischemic heart disease with therapies aimed at inducing BM-PC mobilization and suggest NGF as an important additional therapeutic factor that can contribute to cardiac repair using local and BM-mediated cellular responses. In this context, *Ad*-mediated NGF gene therapy could be considered as a potential therapeutic approach in the setting of ischemic heart diseases. To date, the majority of gene therapy clinical has been based on *Ad* vectors (http://www.wiley.co.uk/genmed/clinical). Due to their high GT efficiency, viral vectors remain the most promising GT agents. In particular, *Ad* vectors represent one of the best viral vector candidate for human gene therapy approaches, as they have a high transduction efficiency, can be produced at high titer, and very rarely integrate into the host genome, thus reducing the risk of insertional mutagenesis.[41] On the other side, their immunogenicity and transient expression may represent a major limitation for *Ad*-mediated gene therapy.[42] Therefore, although their current limitations, *Ad* vectors represent one of the most efficient tools for *in vivo* gene delivery and hold promise for clinical applications requiring a transient transgene expression.

In summary, our data suggest that NGF, through activation of osteoclasts and MMP9 and the release of SCF, stimulates the proliferation of c-kit^{pos} PCs in the BM, thus facilitating PC mobilization into the circulation and their homing to the infarcted heart. In this context, it is important to underline that NGF is a secreted factor and acts extracellularly on its receptor (TrkA), thus any cell type that possess the TrkA receptor can still benefit of its effect.

However, we cannot exclude other potential simultaneous mechanisms whereby NGF might act on BM-PCs, such as regulating catecholamine release through activation of the sympathetic nervous system[43] or activating other key factors involved in BM-PC egress into the circulation (*i.e.*, vascular endothelial growth factor, SDF-1).[9,16] Further investigation will clarify these mechanisms and their relative contributions to post-MI recovery.

MATERIALS AND METHODS

In vivo ***mouse studies.*** Mice were handled in accordance with the Guide for the Care and Use of Laboratory Animals prepared by the Institute of Laboratory Animal Resources and with the prior approval of the UK Home Office and the First Ethical Commission in Warsaw, Poland. Eight to ten-week-old CD1, C57BL/6 (both strains from Harlan, Huntingdon, UK), and *MMP9* KO mice (in a C57BL/6 background originally obtained from Dr. Z. Werb, UCSF, San Francisco, CA) underwent MI induction, as previously described.[15,19] Briefly, mice were anaesthetized (Avertin, 880 mmol/

kg, i.p.; Sigma Aldrich, Poole, UK), orally intubated, and artificially ventilated using a Minivent mouse ventilator (Harvard Apparatus, Kent, UK). The tidal volume was set at 8–9 µl/g and the respiratory rate was set at 140 breaths per minute. Under a surgical microscope, an incision was made at the level of the left fifth intercostal space and MI was induced by permanent ligation of the proximal left anterior descending coronary artery by using a 7.0 Mersilene suture (Ethicon, Somerville, NJ). Coronary occlusion was confirmed by pallor of the LV. GT was performed immediately after induction of MI. Under a surgical microscope, we entered the infarct zone using a 30 G needle bent at the right angle and injected the genetic material in three sites of the MI border zone. Mice were injected in the peri-infarct area (intramyocardially) with an adenoviral vector carrying human NGF (*Ad.hNGF*) at the dose of 10^8 plaque-forming unit (p.f.u.)/15 µl. Control MI mice were injected with an empty vector (*Ad.Null*). Sham-operated mice underwent the same procedure except left anterior descending coronary artery was circled with a 7-0 Mersilene but not occluded. Intramyocardial *Ad.Null* was also delivered to the LV of sham-operated mice. Surgical wounds were sutured and animals were allowed to recover.[15,19]

BM transplantation. For BM transplantation studies, transgenic mice expressing an eGFP cDNA under the control of a chicken β-actin promoter and cytomegalovirus enhancer (C57BL/6-Tg[CAG-EGFP]1Osb/J; Jackson Laboratory, Bar Harbor, ME) were used (n = 2). Recipient mice (4- to 5-week-old C57BL/6 mice; n = 6 mice/group) received whole body irradiation (9.5 Gy), followed by injection of BM cells (1×10^6 eGFP-expressing cells) into the tail vein. After 8 weeks, mice were subjected to MI induction and immediately injected with either *Ad.hNGF* or *Ad.Null* (10^8 p.f.u./15 µl) into the peri-infarct.[15] Sham-operated mice received the same dose of *Ad.Null*.

Preparation of NGF adenoviral vector. As previously described,[15,17] an adenoviral vector carrying human NGF-β (*Ad.hNGF*) was prepared by using the coding sequence for the NGF-β from *p.NGF* amplified (KOD proofreading DNA polymerase; Novagen, Darmstadt, Germany) using the following primers: 5′-GCTAGCGTAATGTCCATGTTGTTCTAC-3′ (NheI site) and 5′-GGATCCTCTCACAGCCT TCCT-3′ (BamHI site). A replication-deficient adenovirus was generated by site-specific Flippase-mediated recombination of the cotransfected shuttle and genomic plasmids in 293 cells. Viral stocks were amplified, CsCl banded, and titrated.

Histology and immunohistochemistry on mouse bones. Femurs and tibiae were collected at 1, 2, 3, and 6 days after surgery. Bones were cleaned from muscles and connective tissues and kept for 24 hours in 10% buffered formalin before being decalcified for 24 hours in 10% formic acid and embedded in paraffin. Bone sections (5 µm in thickness) were prepared into polylysine-coated slides and used for histological or immunohistochemical analyses (n = 5 mice/group/time point). Bones were longitudinally sectioned in order to comprise both epiphysis and diaphysis. Activated osteoclasts were detected by TRAP staining (acid phosphatase, Leukocyte kit; Sigma Aldrich). Sections were counterstained with hematoxylin. Osteoclasts were identified as TRAP-positive cells adjacent to bone surfaces.[44] The number of osteoclasts was quantified (×20 magnification) and expressed as osteoclasts number per centimeter of bone perimeter. TRAP staining was evaluated in one bone section/mouse; 5.0 ± 1.7 cm of linear bone length per mouse was analyzed. Immunohistochemical staining for MMP2 and MMP9 were performed with polyclonal anti-MMP2 (1:5,000) and anti-MMP9 (1:800) antibodies (Abcam, Cambridge, UK) and revealed by the REAL EnVision Detection System, Peroxidase/DAB (Dako, Stockport, UK). The number of MMP2- and MMP9-positive cells was analyzed (×20 magnification) and expressed as MMP-positive cells/mm^2. MMP2 and MMP9 were evaluated in two bone sections/mouse; 12.1 ± 4.5 mm^2 (for MMP2) and 12.5 ± 4.3 mm^2 (for MMP9) of BM parenchyma per mouse was analyzed. Mouse c-kit (1:50; R&D Systems, Abingdon, UK) and CD45 antigens (1:10; Santa Cruz Biotechnology, Santa Cruz, CA) were used to identify hematopoietic PCs, Ki67 (1:500; Abcam) was used to verify the frequency of cycling c-kit^{pos} cells, and CD146 (1:20; Abcam) to identify the BM vascular niche. Sections were visualized using a fluorescent microscope (×20 magnification). The number of c-kit^{pos}, c-kit^{pos}/CD45^{pos}, and c-kit^{pos}/CD45$^{low/neg}$ cells was expressed as positive cells/10^6 BM cells. C-kit^{pos} cells in the BM vascular niche were expressed as number of positive cells for c-kit in proximity to the vascular niche (positive for CD146). Proliferating c-kit cells were expressed as percentage of double-positive cells for c-kit and Ki67. Appropriate nonimmune IgG were used to generate negative controls. For these staining, two bone sections/mouse were employed and 12.0 ± 3.9 mm^2 of BM parenchyma per mouse was analyzed; c-kit^{pos} cells lining the BM endosteal region were assessed in 3.8 ± 3.0 cm of linear bone length per mouse.

ELISA on BM supernatants. Femurs and tibiae (n = 4 mice/group/time point) were flushed in 0.5 ml of phosphate-buffered saline. After spinning, the BM supernatant was collected to perform ELISA assay for human and mouse NGF (PeproTech, London, UK) and mouse SCF (R&D Systems), following manufacturer's instruction.

Immunocytochemistry on mouse BM c-kit^{pos} cells. BM cells were isolated from femurs and tibiae of healthy mice (n = 3) by flushing with 2 ml of endothelial basal medium-2 (Lonza, Slough, UK). Cells were labeled with c-kit monoclonal antibody conjugated with magnetic beads (Miltenyi Biotec, Bisley, UK) and c-kit^{pos} cells were selected by using magnetic-activated cell sorting separation columns (Miltenyi Biotec) according to the manufacture instructions. C-kit^{pos} cells were cytospinned to glass slides (500 rpm for 5 minutes) and fixed with 4% paraformaldehyde. Double staining for c-kit (1:50; R&D Systems; secondary antibody: Alexa-568 donkey anti-goat) and TrkA (1:50; Santa Cruz Biotechnology; secondary antibody: Alexa-488 goat anti-rabbit) was performed. Positive staining was visualized using a fluorescent microscope.

MNCs-osteoclasts differentiation. BM cells from healthy C57BL/6 mice (n = 3) were collected by flushing femurs and tibiae with 2 ml of alpha-Minimum Essential Media (Lonza). Cells were plated overnight in alpha-Minimum Essential Media supplemented with 250 IU penicillin and 250 µg streptomycin in order separate stromal cells (that adhere to the plate) from nonadherent MNCs. Nonadherent MNCs were then cultured (1×10^6 cells/well in a 24-well plate) for 6 days in alpha-minimum essential medium supplemented with M-CSF (10 ng/ml; PeproTech) and RANKL (50 ng/ml; PeproTech) (both required for osteoclasts differentiation from MNCs). Next, immunohistochemistry for TrkA was performed to identify the presence of NGF high-affinity receptor on differentiated osteoclasts. Briefly, differentiated cells were fixed with 4% paraformaldehyde, permeabilized with 0.1% Triton-X, and stained with TrkA (1:50; Santa Cruz Biotechnology; secondary antibody: Alexa-488 goat anti-rabbit). Nuclei were identified by 4′,6-diamidino-2-phenylindole. In order to evaluate the NGF-induced formation of TRAP^{pos} cells from MNCs, in a separate set of experiments, cultured MNCs (1×10^6 cells/well in a 24-well plate) were supplemented for 6 days with M-CSF alone or in combination with NGF (10, 50, or 100 ng/ml; Millipore, Watford, UK) before being submitted to TRAP staining. For these experiments, RANKL was omitted since NGF has been shown to induce RANKL-independent formation of TRAP^{pos} cells.[34]

Flow cytometry analyses in mouse tissues. Evaluation of Lin^{neg}/c-kit^{pos} cells was performed by flow cytometry in mouse PB, BM, and LV at 3 days postoperation (n = 5 mice/group), as previously described.[15] Mice were anesthetized (Avertin) and PB was collected by cardiac puncture. Next, hearts were harvested and blood was washed out with phosphate-buffered saline. The LV was separated from right ventricle and septum, weighted, and minced. A "myocyte-depleted" cardiac cell population was prepared by enzymatic digestion of LV in 0.1% collagenase IV (30 minutes at 37 °C) and filtration through a 70-µm mesh. Total BM cells were flushed out from femurs and tibiae (additionally collected from the same mice) with 2 ml of Endothelial Basal Medium-2 (Lonza). The expression of

c-kit (APC-Cy7 conjugated; BD Biosciences, Oxford, UK) was evaluated in isolated cells stained for anti-lineage markers antibodies (FITC conjugated; Caltag, Buckingham, UK). Evaluation of Lin^{neg}/c-kit^{pos}/GFP^{pos} cells was performed on mouse LV of chimeric mice at 3 days after surgery and GT. In order to assess the efficacy of BM transplantation, flow cytometry for GFP was also performed in PB collected by tail puncture at 8 weeks after GFP-BM cells transplantation. Unstained and single-stained controls were performed to define positivity. Fluorescence was analyzed in a Canto II flow cytometer using the Diva software (BD). Lin^{neg}/c-kit^{pos} cells were expressed as percentage of total BM or PB cells. In order to determine the absolute number of PC populations per gram of heart, flow cytometry analyses were performed using fluorescent counting beads (Invitrogen, Paisley, UK). Following manufacturer instruction, 20,000 counting beads in 100 µl (same volume as sample) were added to the myocardial sample immediately before use. The final absolute count was determined by the formula: final absolute count = ((number of cells counted/total number of beads counted) × number of beads per ml)/mg of LV tissue.

Flow cytometry in human PB samples. Experimental procedures involving human subjects were performed in accordance with the Declaration of Helsinki and were approved by the responsible ethics committees. Research on clinical samples was performed in agreement with the Human Tissue Act (HTA). MNCs were isolated from PB (15 ml) obtained by vein puncture from a forearm vein of healthy volunteers (n = 11) and patients with acute MI (n = 11, provided by Dr. Marco Valgimigli, Cardiology Department, University of Ferrara, Ferrara, Italy) participating in a registered prospective clinical study (NCT01271309) at Ferrara University Hospital (Ferrara, Italy).[25] All MI patients underwent percutaneous coronary intervention immediately after admission to the hospital and prior to sampling for use in the current study.

Inclusion criteria. acute MI was defined as chest pain at rest lasting at least 20 minutes, transient or persistent ST segment ischemic ECG changes, and high levels of the cardiac necrosis markers creatine phosphokinase-muscle band and troponin. Optimal treatment included all drugs recommended by international guidelines except for statins, which were commenced only after collection of samples necessary to the study to avoid the confounding effect of these drugs on PC counting.

Exclusion criteria. Age below 18 years, anemia, hemodynamic instability, systolic blood pressure <90 mmHg, alterations in hematopoiesis, cancer, and lack of consent to participate to the study.

MNCs were isolated by density centrifugation on Histopaque 1077 (Sigma Aldrich, Milan, Italy) and stained for the hematopoietic PCs antigen CD34 (FITC conjugated; Miltenyi Biotec, Bologna, Italy) in combination with c-kit (APC conjugated; R&D Systems) and TrkA (PE conjugated; R&D Systems). CD34/c-kit/TrkA–positive cells were evaluated by flow cytometry and expressed as a percentage of total MNCs. Fluorescence was analyzed in a Canto II flow cytometer using the Diva software.

Transwell migration assay on human BM cells. Experimental procedures involving human subjects were performed in accordance with the Declaration of Helsinki and were approved by the responsible ethics committees. Research on clinical samples was performed in agreement with the HTA.

Anonymized BM leftover samples were obtained from noncardiovascular patients (n = 3) undergoing hip replacement surgery at the Bristol Southmead Hospital (provided by Prof. Ashley Blom, Orthopaedic Surgery, Musculoskeletal Research Unit, University of Bristol, Bristol, UK). BM samples were collected as part of routine total hip replacement for osteoarthritis. All patients did consent and samples were provided anonymously to the research staff by the clinical staff. Briefly, the femoral neck was resected and a broach inserted into the proximal femur. The broach caused the displacement of marrow from the femoral canal and the marrow, commonly discarded, was collected and placed in sterile falcon tubes. The BM was then transferred into new falcon tubes containing phosphate-buffered saline with 5 mmol/l ethylenediaminetetraacetic acid. MNCs were isolated by density centrifugation on Histopaque 1077 (Sigma Aldrich). MNCs were resuspended in Endothelial Basal Medium-2 and seeded (6×10^6) on the upper part of six-transwell plate filters (pore size: 3 µm). Endothelial Basal Medium-2 supplemented with NGF (100 ng/ml; Millipore) alone or in combination with the TrkA inhibitor K252a (100 nmol/l; Sigma Aldrich) was placed in the lower wells. SDF-1 (100 ng/ml; eBiosciences, Hatfield, UK) and bovine serum albumin (Sigma Aldrich) were used as positive and negative controls, respectively. After overnight incubation, migrated and nonmigrated cells were collected and stained for the hematopoietic PCs antigen CD34 (FITC conjugated; Miltenyi Biotec, Bisley, UK) in combination with c-kit (APC conjugated; R&D Systems) and TrkA (PE conjugated; R&D Systems). Total MNCs, as well as CD34/c-kit– and CD34/c-kit/TrkA–positive cells were evaluated by flow cytometry and expressed as a ratio of migrated to nonmigrated cells. Fluorescence was analyzed in a Canto II flow cytometer using the Diva software.

Statistical analyses. Values are presented as mean ± SEM. Statistical significance was evaluated through the use of an unpaired t-test for comparisons between two groups. For comparison among more than two groups, one-way analysis of variance was used, followed by Bonferroni *post hoc* test. Analyses were performed using the SigmaStat 3.1 software. A P value <0.05 was interpreted to denote statistical significance.

SUPPLEMENTARY MATERIAL

Table S1. Characteristics of acute MI patients and control subjects.

ACKNOWLEDGMENTS

A.C. is a British Heart Foundation (BHF) Intermediate Research fellow; G.D.A. is a BHF Chair in Cardiac Surgery and a NIHR senior investigator; C.E. is a BHF Senior Research Fellow.

We are grateful to Ashley Blom (University of Bristol) for providing human BM samples, Atsuhiko Oikawa (University of Bristol) for help in setting up the BM transplantation model in mice, and to Graciela Sala-Newby (University of Bristol) for help with MMP9 assessment. We acknowledge the help provided by Agnieszka Jazwa and Jozef Dulak (Jagiellonian University, Krakow, Poland), who provided equipment for performing experiments on murine colonies in Poland.

This study was supported by the BHF Senior Research Fellowship to C.E., the BHF Centre for Vascular Regeneration (BHF-CVR), and the National Institute of Health Research (NIHR) Bristol Cardiovascular Biomedical Research Unit. The views expressed are those of the authors and not necessarily those of the NHS, the NIHR, or the Department of Health.

REFERENCES

1. Kollet, O, Dar, A, Shivtiel, S, Kalinkovich, A, Lapid, K, Sztainberg, Y *et al.* (2006). Osteoclasts degrade endosteal components and promote mobilization of hematopoietic progenitor cells. *Nat Med* **12**: 657–664.
2. Adams, GB and Scadden, DT (2006). The hematopoietic stem cell in its place. *Nat Immunol* **7**: 333–337.
3. Kollet, O, Dar, A and Lapidot, T (2007). The multiple roles of osteoclasts in host defense: bone remodeling and hematopoietic stem cell mobilization. *Annu Rev Immunol* **25**: 51–69.
4. Frangogiannis, NG, Smith, CW and Entman, ML (2002). The inflammatory response in myocardial infarction. *Cardiovasc Res* **53**: 31–47.
5. Takahashi, T, Kalka, C, Masuda, H, Chen, D, Silver, M, Kearney, M *et al.* (1999). Ischemia- and cytokine-induced mobilization of bone marrow-derived endothelial progenitor cells for neovascularization. *Nat Med* **5**: 434–438.
6. Guo, J, Jie, W, Shen, Z, Li, M, Lan, Y, Kong, Y *et al.* (2014). SCF increases cardiac stem cell migration through PI3K/AKT and MMP-2/-9 signaling. *Int J Mol Med* **34**: 112–118.
7. Harada, M, Qin, Y, Takano, H, Minamino, T, Zou, Y, Toko, H *et al.* (2005). G-CSF prevents cardiac remodeling after myocardial infarction by activating the Jak-Stat pathway in cardiomyocytes. *Nat Med* **11**: 305–311.
8. Sugiyama, T, Kohara, H, Noda, M and Nagasawa, T (2006). Maintenance of the hematopoietic stem cell pool by CXCL12-CXCR4 chemokine signaling in bone marrow stromal cell niches. *Immunity* **25**: 977–988.
9. Moore, MA, Hattori, K, Heissig, B, Shieh, JH, Dias, S, Crystal, RG *et al.* (2001). Mobilization of endothelial and hematopoietic stem and progenitor cells by adenovector-mediated elevation of serum levels of SDF-1, VEGF, and angiopoietin-1. *Ann NY Acad Sci* **938**: 36–45; discussion 45.
10. Hattori, K, Dias, S, Heissig, B, Hackett, NR, Lyden, D, Tateno, M *et al.* (2001). Vascular endothelial growth factor and angiopoietin-1 stimulate postnatal hematopoiesis by recruitment of vasculogenic and hematopoietic stem cells. *J Exp Med* **193**: 1005–1014.

11. Kollet, O, Shivtiel, S, Chen, YQ, Suriawinata, J, Thung, SN, Dabeva, MD *et al.* (2003). HGF, SDF-1, and MMP-9 are involved in stress-induced human CD34+ stem cell recruitment to the liver. *J Clin Invest* **112**: 160–169.
12. Heissig, B, Hattori, K, Dias, S, Friedrich, M, Ferris, B, Hackett, NR *et al.* (2002). Recruitment of stem and progenitor cells from the bone marrow niche requires MMP-9 mediated release of kit-ligand. *Cell* **109**: 625–637.
13. Fuller, K, Kirstein, B and Chambers, TJ (2007). Regulation and enzymatic basis of bone resorption by human osteoclasts. *Clin Sci (Lond)* **112**: 567–575.
14. Delaissé, JM, Andersen, TL, Engsig, MT, Henriksen, K, Troen, T and Blavier, L (2003). Matrix metalloproteinases (MMP) and cathepsin K contribute differently to osteoclastic activities. *Microsc Res Tech* **61**: 504–513.
15. Meloni, M, Caporali, A, Graiani, G, Lagrasta, C, Katare, R, Van Linthout, S *et al.* (2010). Nerve growth factor promotes cardiac repair following myocardial infarction. *Circ Res* **106**: 1275–1284.
16. Emanueli, C, Salis, MB, Pinna, A, Graiani, G, Manni, L and Madeddu, P (2002). Nerve growth factor promotes angiogenesis and arteriogenesis in ischemic hindlimbs. *Circulation* **106**: 2257–2262.
17. Caporali, A, Sala-Newby, GB, Meloni, M, Graiani, G, Pani, E, Cristofaro, B *et al.* (2008). Identification of the prosurvival activity of nerve growth factor on cardiac myocytes. *Cell Death Differ* **15**: 299–311.
18. Boyle, WJ, Simonet, WS and Lacey, DL (2003). Osteoclast differentiation and activation. *Nature* **423**: 337–342.
19. Meloni, M, Marchetti, M, Garner, K, Littlejohns, B, Sala-Newby, G, Xenophontos, N *et al.* (2013). Local inhibition of microRNA-24 improves reparative angiogenesis and left ventricle remodeling and function in mice with myocardial infarction. *Mol Ther* **21**: 1390–1402.
20. Asagiri, M and Takayanagi, H (2007). The molecular understanding of osteoclast differentiation. *Bone* **40**: 251–264.
21. Ashman, LK (1999). The biology of stem cell factor and its receptor C-kit. *Int J Biochem Cell Biol* **31**: 1037–1051.
22. Smith, MA, Court, EL and Smith, JG (2001). Stem cell factor: laboratory and clinical aspects. *Blood Rev* **15**: 191–197.
23. Khan, KM, Falcone, DJ and Kraemer, R (2002). Nerve growth factor activation of Erk-1 and Erk-2 induces matrix metalloproteinase-9 expression in vascular smooth muscle cells. *J Biol Chem* **277**: 2353–2359.
24. Dagnell, C, Kemi, C, Klominek, J, Eriksson, P, Sköld, CM, Eklund, A *et al.* (2007). Effects of neurotrophins on human bronchial smooth muscle cell migration and matrix metalloproteinase-9 secretion. *Transl Res* **150**: 303–310.
25. Fortunato, O, Spinetti, G, Specchia, C, Cangiano, E, Valgimigli, M and Madeddu, P (2013). Migratory activity of circulating progenitor cells and serum SDF-1α predict adverse events in patients with myocardial infarction. *Cardiovasc Res* **100**: 192–200.
26. Simari, RD, Pepine, CJ, Traverse, JH, Henry, TD, Bolli, R, Spoon, DB *et al.* (2014). Bone marrow mononuclear cell therapy for acute myocardial infarction: a perspective from the cardiovascular cell therapy research network. *Circ Res* **114**: 1564–1568.
27. Moazzami, K, Roohi, A and Moazzami, B (2013). Granulocyte colony stimulating factor therapy for acute myocardial infarction. *Cochrane Database Syst Rev* **5**: CD008844.
28. Beohar, N, Rapp, J, Pandya, S and Losordo, DW (2010). Rebuilding the damaged heart: the potential of cytokines and growth factors in the treatment of ischemic heart disease. *J Am Coll Cardiol* **56**: 1287–1297.
29. Kang, HJ, Kim, HS, Zhang, SY, Park, KW, Cho, HJ, Koo, BK *et al.* (2004). Effects of intracoronary infusion of peripheral blood stem-cells mobilised with granulocyte-colony stimulating factor on left ventricular systolic function and restenosis after coronary stenting in myocardial infarction: the MAGIC cell randomised clinical trial. *Lancet* **363**: 751–756.
30. Steinwender, C, Hofmann, R, Kammler, J, Kypta, A, Pichler, R, Maschek, W *et al.* (2006). Effects of peripheral blood stem cell mobilization with granulocyte-colony stimulating factor and their transcoronary transplantation after primary stent implantation for acute myocardial infarction. *Am Heart J* **151**: 1296.e7–1296.13.
31. Wright, DE, Wagers, AJ, Gulati, AP, Johnson, FL and Weissman, IL (2001). Physiological migration of hematopoietic stem and progenitor cells. *Science* **294**: 1933–1936.
32. Lapid, K, Glait-Santar, C, Gur-Cohen, S, Canaani, J, Kollet, O and Lapidot, T (2008). *Egress and Mobilization of Hematopoietic Stem and Progenitor Cells: A Dynamic Multi-Facet Process*. StemBook: Cambridge (MA).
33. Hattersley, G, Owens, J, Flanagan, AM and Chambers, TJ (1991). Macrophage colony stimulating factor (M-CSF) is essential for osteoclast formation *in vitro*. *Biochem Biophys Res Commun* **177**: 526–531.
34. Hemingway, F, Taylor, R, Knowles, HJ and Athanasou, NA (2011). RANKL-independent human osteoclast formation with APRIL, BAFF, NGF, IGF I and IGF II. *Bone* **48**: 938–944.
35. Levi-Montalcini, R and Angeletti, PU (1968). Nerve growth factor. *Physiol Rev* **48**: 534–569.
36. Conti, AM, Fischer, SJ and Windebank, AJ (1997). Inhibition of axonal growth from sensory neurons by excess nerve growth factor. *Ann Neurol* **42**: 838–846.
37. Aicher, A, Kollet, O, Heeschen, C, Liebner, S, Urbich, C, Ihling, C *et al.* (2008). The Wnt antagonist Dickkopf-1 mobilizes vasculogenic progenitor cells *via* activation of the bone marrow endosteal stem cell niche. *Circ Res* **103**: 796–803.
38. Fragkouli, A, Tzinia, AK, Charalampopoulos, I, Gravanis, A and Tsilibary, EC (2011). Matrix metalloproteinase-9 participates in NGF-induced α-secretase cleavage of amyloid-β protein precursor in PC12 cells. *J Alzheimers Dis* **24**: 705–719.
39. Blanco-Mezquita, T, Martinez-Garcia, C, Proença, R, Zieske, JD, Bonini, S, Lambiase, A *et al.* (2013). Nerve growth factor promotes corneal epithelial migration by enhancing expression of matrix metalloprotease-9. *Invest Ophthalmol Vis Sci* **54**: 3880–3890.
40. Iwakura, A, Shastry, S, Luedemann, C, Hamada, H, Kawamoto, A, Kishore, R *et al.* (2006). Estradiol enhances recovery after myocardial infarction by augmenting incorporation of bone marrow-derived endothelial progenitor cells into sites of ischemia-induced neovascularization *via* endothelial nitric oxide synthase-mediated activation of matrix metalloproteinase-9. *Circulation* **113**: 1605–1614.
41. Lopez-Gordo, E, Podgorski, II, Downes, N and Alemany, R (2014). Circumventing antivector immunity: potential use of nonhuman adenoviral vectors. *Hum Gene Ther* **25**: 285–300.
42. Chen, P, Kovesdi, I and Bruder, JT (2000). Effective repeat administration with adenovirus vectors to the muscle. *Gene Ther* **7**: 587–595.
43. Récalde, A, Richart, A, Guérin, C, Cochain, C, Zouggari, Y, Yin, KH *et al.* (2012). Sympathetic nervous system regulates bone marrow-derived cell egress through endothelial nitric oxide synthase activation: role in postischemic tissue remodeling. *Arterioscler Thromb Vasc Biol* **32**: 643–653.
44. Ballanti, P, Minisola, S, Pacitti, MT, Scarnecchia, L, Rosso, R, Mazzuoli, GF *et al.* (1997). Tartrate-resistant acid phosphate activity as osteoclastic marker: sensitivity of cytochemical assessment and serum assay in comparison with standardized osteoclast histomorphometry. *Osteoporos Int* **7**: 39–43.